Atomic and bond topological properties of the tripeptide L-alanyl–L-alanyl–L-alanine based on its experimental charge density obtained at 20 K†‡

E. Rödel,[a] M. Messerschmidt,[a] B. Dittrich[b] and P. Luger*[a]

Received 17th October 2005, Accepted 28th November 2005
First published as an Advance Article on the web 5th January 2006
DOI: 10.1039/b514717d

A 20 K high resolution X-ray data set of L-Ala–L-Ala–L-Ala*1/2 H_2O was measured using an ultra-low temperature laboratory setup, that combines area detection and a closed cycle helium cryostat. The charge density determination includes integration of atomic basins and topological analysis according to Bader's quantum theory of atoms in molecules. Two tripeptide units are found in the asymmetric unit, allowing the assessment of transferability of bond topological and atomic properties taking also into consideration previous data of oligopeptides. With respect to invariom modeling the limits of such transferability are investigated and the results of this study show the validity of the nearest/next-nearest neighbour approximation and support the use of database approaches for electron density modeling of macromolecules.

Introduction

Bader's theory of atoms in molecules[1] (AIM) can be used to determine atomic, bonding and non bonding properties of a chemical system from its charge density $\rho(\boldsymbol{r})$ in a quantitative manner. The charge density can be obtained either theoretically from *ab initio* calculations or experimentally by a multipole refinement of high resolution X-ray diffraction data. Bader's theory furthermore offers a well defined partitioning scheme yielding atoms or functional groups. This procedure makes use of the zero-flux surfaces (ZFS) in the electron density gradient vector field to determine atomic basins around a nuclear attractor of the related trajectories. The atomic basin unambiguously defines the atomic volume of a nuclear attractor within a molecular density. With the atomic volume and shape established, the encircled charge of an atom, and other properties, can be obtained by integration.

In this work the AIM theory is used to compare atomic and bonding properties in a similar chemical environment using experimental data. Regarding their reactivity, functional groups are rather independent from the molecule they are part of. On the electronic level one would expect that the charge density, and derived properties of a functional group composed of its contributing atoms, should possess a high degree of transferability when compared for different molecules.

Assuming that the nearest covalently bonded neighbours of an atom[2] and also the hydrogen bond environment influence the charge density and derived properties of a functional group, or the individual atoms that form it, an open question is the limit of this transferability. This question is essential for the application of database approaches[3–5] to model the electron density of larger systems. The title compound, a tripeptide formed only by alanine residues, allows one to study whether or not an atom's next nearest neighbours influences its covalent bonding electron density.

High resolution X-ray data collection and multipole refinement

Two crystalline forms of the tripeptide L-alanyl–L-alanyl–L-alanine (trialanine) are known in the literature. One is solvent free,[6] the second one contains water in the crystal structure. The latter form, the subject of this study (see Fig. 1), is known to have two crystallographically independent molecules of trialanine and one water molecule in the asymmetric unit.[7] The water is found on two sites of twofold axes. A needle shaped crystal was cut to 0.3 × 0.4 × 0.5 mm, glued on a beryllium needle and protected in a glass capillary of 0.5 mm diameter. The beryllium needle is needed to improve temperature conduction to the crystal.

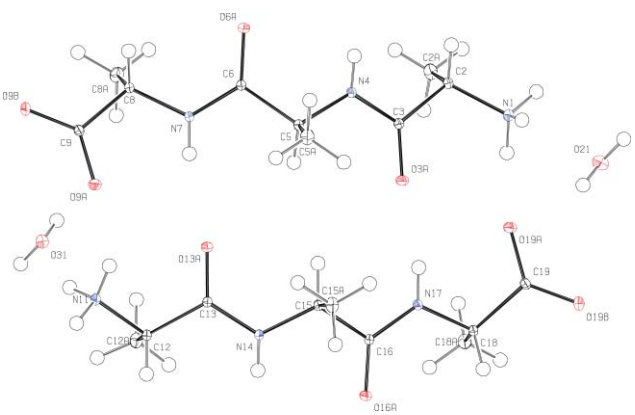

Fig. 1 ORTEP[8] representation of the asymmetric unit with atomic numbering scheme. Displacement ellipsoids drawn at a 50% probability.

Data collection was performed with Mo Kα radiation (graphite monochromation) at 20 K on a Huber four-circle diffractometer equipped with a Bruker APEX-CCD area detector and a closed-cycle helium cryostat. A 0.1 mm Kapton film cylinder was used as vacuum chamber as described in ref. 9. Data reduction was

[a]*Institut für Chemie/Kristallographie der Freien Universität Berlin, Takustr. 6, Berlin, D-14195, Germany. E-mail: luger@chemie.fu-berlin.de*
[b]*Chemistry M313, School of Biological and Molecular Sciences, University of Western Australia, Crawley, 6009, Australia*

† Electronic supplementary information (ESI) available: Experimental backbone torsion angles. See DOI: 10.1039/b514717d

‡ CCDC reference number 286835. For crystallographic data in CIF or other electronic format see DOI: 10.1039/b514717d

performed using SAINT.[10] Spherical refinement with the program SHELXL97,[11] making use of all atoms (including hydrogens) from the room temperature structure[7] as input, led to an *R* value of 2.9%. The data were then interpreted with the multipole formalism[12] using the full-matrix least-squares refinement program XDLSM of the XD[13] suite.

In a multipole refinement the data to parameter ratio should be sufficiently high. However, as it was intended to investigate the question of similarity of atomic properties, the use of chemical constraints was strongly limited so that it did not include *a priori* information in the modeling. Hence chemical constraints were assumed only for the hydrogen atoms and their distances to their corresponding parent heavy atoms were fixed standard neutron values. For the heavier atoms the following site symmetry was introduced: *m* symmetry for C in the carboxylate group, C and N in the peptide bond and 3-fold symmetry for C in methyl groups. The residual density after refinement is practically featureless (see Fig. 2) indicating a proper representation of the experimental density by the multipole model. *R* values and related data for multipole refinement are summarized in Table 1.

Theoretical calculations

For a comparison with the experimental results, electron densities were also derived theoretically from *ab initio* calculations. GAUSSIAN98[14] was used for single point calculations using HF/6-311 + + G(*d*,*p*) and B3LYP/6-311 + + G(*d*,*p*) basis sets for the experimental geometry of trialanine. The resulting wave functions were analysed with the programs MORPHY98[15] and MOLDEN.[16]

Table 1 Multipole refinement details of trialanine

N_{ref} ($F_o > 4\sigma(F_o)$)	12928
N_v	988
R_F	0.0183
R_{all}	0.0247
R_{wF}	0.0153
R_{F2}	0.0264
R_{allF2}	0.0279
R_{wF2}	0.0303
Gof	0.67
N_{ref}/N_v	13.1

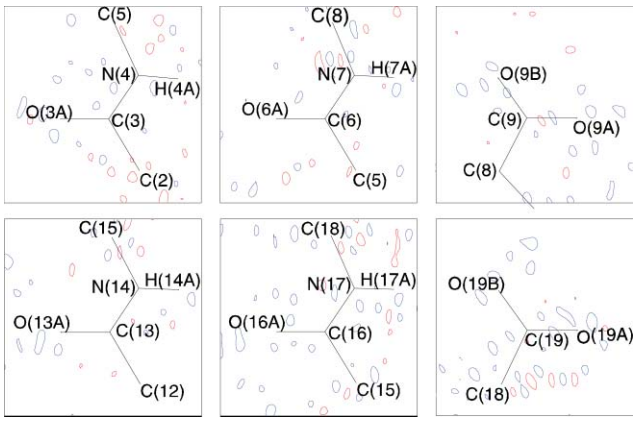

Fig. 2 Residual density maps in the planes of the peptide bonds and the carboxylate groups. Contour intervals 0.1 eÅ^{-3}, blue positive, red negative.

Results and discussion

Molecular and crystal structure

The conformations of the two crystallographically independent molecules are basically alike. As usually found in peptide crystal structures, the tripeptide is zwitterionic, and hence carries charges on the terminal groups. This favours the arrangement of trialanine molecules in a β-sheet type head-to-tail packing in the crystal. In the lattice, oxygen atoms of the water molecules are located on a twofold axis and thus two half molecules formally add up to one water molecule.

The peptide backbone torsion angles differ by at most 26° between the two independent molecules (see the electronic supplementary information (ESI)†), except for the conformation of the terminal ammonium group, being staggered in one molecule and eclipsed in the second. In the asymmetric unit, 12 hydrogen bonds according to the 12 potential N–H and O–H donor groups were found (Table 2). The peptide groups of both molecules lie roughly in a common plane close to the crystallographic *ac*-plane and are connected *via* hydrogen bonds. Stability in other directions is established by hydrogen bonds *via* water molecules (see also Fig. 3).

Charge density and topological analysis

For a quantitative description of the electronic structure a full topological analysis was carried out with the XDPROP program

Table 2 Summary of hydrogen bonds including geometric and bond topological properties (ρ and$\nabla^2\rho$ in *e* Å^{-3} and *e* Å^{-5} respectively, distances and angles in Å and deg, E_{HB} in kJ mol^{-1})

D–H···A	Sym./transl.	$\rho(\mathbf{r})$	$\nabla^2\rho(\mathbf{r})$	H···A	D···A	D–H···A	E_{HB}
N(1)–H(1A)···O(19B)	$1-x, y, 1-z$	0.28	4.60	1.68	2.6995(5)	167	59.8
N(1)–H(1B)···O(19A)	x, y, z	0.25	4.05	1.73	2.7607(7)	175	49.9
N(1)–H(1C)···O(21)	x, y, z	0.13	2.22	2.03	2.8457(5)	134	17.0
N(4)–H(4A)···O(16A)	$-\frac{1}{2}+x, -\frac{1}{2}+y, z$	0.15	2.94	1.90	2.8835(5)	163	27.1
N(7)–H(7A)···O(13A)	x, y, z	0.13	2.42	1.98	2.9432(6)	158	20.3
O(31)–H(31A)···O(9A)	x, y, z	0.24	4.94	1.68	2.6360(7)	168	59.8
N(11)–H(11A)···O(9A)	x, y, z	0.13	2.52	1.95	2.8767(7)	148	22.6
N(11)–H(11B)···O(31)	$x, 1+y, z$	0.20	4.02	1.77	2.7854(6)	168	43.2
N(11)–H(11C)···O(9B)	$1-x, y, -z$	0.28	4.97	1.67	2.6872(6)	167	61.9
N(14)–H(14A)···O(6A)	$\frac{1}{2}+x, \frac{1}{2}+y, z$	0.14	2.89	1.91	2.8754(6)	158	26.1
N(17)–H(17A)···O(3A)	x, y, z	0.09	1.86	2.09	3.0260(6)	153	13.7
O(21)–H(21A)···O(19A)	$1-x, -1+y, 1-z$	0.20	4.02	1.75	2.6929(5)	163	46.5

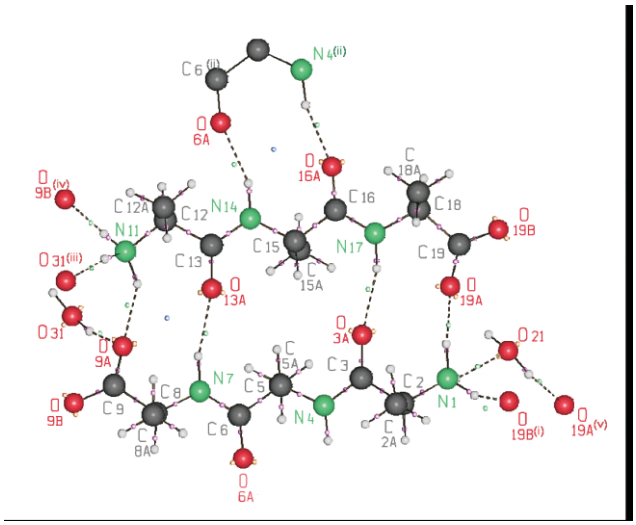

Fig. 3 SCHAKAL[17] representation of the trialanine and water molecules with all hydrogen bonds and with all identified critical points, indicated by the following colour code: (3, −1) BCPS on covalent bonds: rose, on hydrogen bonds: green; (3, +3) critical points of $\nabla^2\rho(\boldsymbol{r})$: orange; (3, +1) ring critical points: blue. Hydrogen bonds: dashed lines. Symmetry related atoms refer to the following symmetry operations (see also Table 2): (i) 1 $-x,y,1-z$; (ii) $1/2+x,1/2+y,z$; (iii) $x,1+y,z$; (iv) $1-x,y,-z$; (v) $1-x,-1+y,1-z$.

of the XD package. Various types of critical point (CPs) were identified illustrated by different colour codes in Fig. 3. (3, −1) bond critical points (BCPs) were found for all covalent bonds (rose colours in Fig. 3) and on the hydrogen bonds (green colour). In addition (3, +3) critical point of $\nabla^2\rho(\boldsymbol{r})$ in the oxygen lone pair region (orange) are seen in Fig. 3, they will be discussed later. The hydrogen bonding pairs in the peptide regions establish three formal ten membered ring structures and in two of them (3, +1) ring critical points of low electron density (0.016 and 0.030 eÅ^{-3}) were identified (shown in blue).

Before we average the topological properties for similar bonds we would like to assess the limits of transferability. With respect to the recently introduced invariom concept the question to which extent topological and atomic properties of molecular fragments are transferable is of special interest.[5,18] For studying this question the title compound is well suited in that on one hand the data of the two independent molecules can be compared with respect to the influence of hydrogen bonding. On the other hand the alanine residue exists in three forms: the first is the N-terminus with the positively charged ammonium group, the second is the central fragment, which is a common building block in polypeptides, while the third form of the fragment is the C-terminus with the negatively charged carboxylate group. Two peptide bonds link the three residues. If a significant influence of the charged groups on the peptide linkage was detectable, a next nearest neighbour influence should manifest itself in different topological properties of the two peptide bonds and the atomic properties of the participating atoms. Table 3 compares $\rho(\boldsymbol{r}_{BCP})$ and $\nabla^2\rho(\boldsymbol{r}_{BCP})$ values for the individual C–C and C–N bonds of the three residues.

When we focus on the C_α atom and the bonds to its neighbouring atoms we observe a difference between partly double bond types of C_α and C_α–NH_3^+ (Table 3). This is to be expected because the nearest neighbours of an ammonium nitrogen and a peptide

Table 3 Bond topological properties of C–C and C–N bonds with various neighbours. The type of one of the neighbour atoms not directly involved in the bond is given in parentheses (in e Å^{-3} and in e Å^{-5}, respectively)

Bond type	Bond	$\rho(\boldsymbol{r})$	$\nabla^2\rho(\boldsymbol{r})$
(N_{amm})–C_α–C_{pep}	C(2)–C(3)	1.74(4)	−11.3(2)
	C(12)–C(13)	1.76(4)	−11.7(2)
	Average	*1.75*	*−11.5*
(N_{pep})–C_α–C_{pep}	C(5)–C(6)	1.64(4)	−9.0(2)
	C(15)–C(16)	1.72(4)	−13.1(2)
	Average	*1.68*	*−11.0*
(N_{pep})–C_α–C_{carbox}	C(8)–C(9)	1.79(4)	−11.5(2)
	C(18)–C(19)	1.77(4)	−10.9(2)
	Average	*1.78*	*−11.2*
N_{amm}–C_α–(C_{pep})	N(1)–C(2)	1.83(4)	−14.2(2)
	N(11)–C12)	1.69(4)	−8.3(2)
	Average	*1.76*	*−11.3*
N_{pep}–C_α–(C_{pep})	N(4)–C(5)	1.82(4)	−9.4(2)
	N(14)–C(15)	1.88(4)	−13.2(2)
	Average	*1.85*	*−11.3*
N_{pep}–C_α–(C_{carbox})	N(7)–C(8)	1.80(4)	−10.7(2)
	N(17)–C(18)	1.80(4)	−10.9(2)
	Average	*1.80*	*−10.8*
(NH_3)–C_α–C_β	C(2)–C(2A)	1.59(4)	−8.4(2)
	C(12)–C(12A)	1.61(4)	−9.4(2)
	Average	*1.60*	*−8.9*
(N_{pep})–C_α–C_β	C(5)–C(5A)	1.58(4)	−7.2(1)
	C(15)–C(15A)	1.62(3)	−10.0(1)
	Average	*1.60*	*−9.1*
(C_{carbox})–C_α–C_β	C(8)–C(8A)	1.59(4)	−9.0(2)
	C(18)–C(18A)	1.61(4)	−10.2(1)
	Average	*1.60*	*−9.6*
N_{pep}–C_{pep}–$(C_\alpha$–$NH_3)$	C(3)–N(4)	2.39(4)	−23.3(2)
	C(13)–N(14)	2.43(4)	−21.9(2)
	Average	*2.41*	*−22.6*
$(C_{carbox}$–$C_\alpha)$–N_{pep}–C_{pep}	C(6)–N(7)	2.43(4)	−22.0(2)
	C(16)–N(17)	2.45(4)	−24.8(2)
	Average	*2.44*	*−23.4*

bond nitrogen differ. In an invariom transfer this difference can be accounted for as two different invariom (N1c1h1h1h+ and N1.5c[1.5o1c]1c1h) would be used. If a next nearest neighbour influence existed, it should also be detectable by differences in bond topological properties. Assuming a next nearest neighbour influence we would expect a difference also in the C_α–C_β bond strength. Here no influence is detectable, or, at least smaller than the experimental inaccuracy of a high resolution state of the art study.

Averages of the topological descriptors of different bond types, assuming there is no next-next nearest neighbour influence, are summarized in Table 4, which lists also the corresponding values from the HF and B3LYP calculations. Theoretically derived $\rho(\boldsymbol{r}_{BCP})$ values are systematically lower for polar C–O and C–N bonds. C–C bonds are in the same range for theory and experiment. This is a frequently observed trend in charge density work and has, for example, recently been expressed by Hibbs *et al.*[19] Mean deviation between experiment and B3LYP is 0.14(9) e Å^{-3} and for experiment/HF 0.14(7) e Å^{-3}. For the Laplacians the variations are higher.

Further comparison is made in Table 4 with averages of previous studies on a number of amino acids, oligo- and pseudopeptides.[20–23] Provided that the statistical spread for experimental averages is 0.01–0.07 e Å^{-3} for $\rho(\boldsymbol{r}_{BCP})$ and 0.7–4 e Å^{-5} for $\nabla^2\rho(\boldsymbol{r}_{BCP})$ when experimental results for different molecules are compared,[24] a high degree of transferability can be deduced from the various

Table 4 Averaged $\rho(\boldsymbol{r}_{BCP})$ (first line) and $\nabla^2\rho(\boldsymbol{r}_{BCP})$ (second line) values (in e Å^{-3} and e Å^{-5}, respectively) for the different bond types in trialanine from experiment and theory. Related data from literature are also given for comparison

	Theory		Experiment				
Bond	B3LYP/6-311 + + G(*d*,*p*)	HF/6-311 + + G(*d*,*p*)	Trialanine	Peptides[22]	Peptides[20]	Ala[23]	Amino acids[21]
$N_{peptide}$–$C_{peptide}$	2.29(1)	2.33(1)	2.43(3)	2.39(8)	2.4	—	—
	−23.7(2)	−23.4(7)	−23(1)	−23.3(21)	−23.4	—	—
C_α–$N_{peptide}$	1.69(1)	1.67(1)	1.76(4)	1.84(6)	1.8	—	—
	−14.0(1)	−6.9(2)	11(2)	−13.22(16)	−10.2	—	—
C_α–$C_{peptide}$	1.71(1)	1.81(1)	1.71(5)	1.77(4)	1.70	—	—
	−14.6(2)	−18.9(2)	−11(2)	−15(2)	−12.7	—	—
$C_{peptide}$–$O_{peptide}$	2.65(2)	2.68(2)	2.87(4)	3.0(1)	2.8	—	—
	−10.2(1)	−6.9(1)	−29(3)	−36(6)	−26.1	—	—
C_α–C_β	1.61(1)	1.70(1)	1.59(2)	1.67(5)	—	1.67	1.68(8)
	−12.8(1)	−16.1(1)	−9(1)	−11(3)	—	−10.1	−12(3)
C_α–$N_{ammonium}$	1.59(1)	1.57(1)	1.76(7)	1.80(6)	—	1.70	1.68(5)
	−12.2(3)	−4.6(9)	−11(4)	−13(2)	—	−11.1	−11(3)
C_α–C_{carbox}	1.69(1)	1.80(1)	1.78(1)	1.73(8)	—	1.76	1.75(6)
	−11.2(3)	−18.8(2)	−11.2(4)	−13(3)	—	−10.8	−14(3)
longer C_{carbox}–O	2.49(1)	2.51(1)	2.72(6)	2.72(9)	—	2.86	2.71(9)
	−12.1(2)	−8.4(2)	−27(4)	−33(5)	—	−29.6	−34(5)
shorter C_{carbox}–O	2.57(1)	2.60(1)	2.82(1)	2.81(1)	—	3.02	2.9(2)
	−11.2(3)	−7.6(5)	−33.1(7)	−36(5)	—	−39.0	−36(4)

average values listed in Table 4. This holds also when $\rho(\boldsymbol{r}_{BCP})$ and $\nabla^2\rho(\boldsymbol{r}_{BCP})$ are compared with results from the experimental charge density study of L-alanine[23] at 23 K. A similar spread of experimental values has previously been found in related studies for these quantities.[18,20–22,24]

Atomic properties and transferability

As mentioned before, Bader's theory of atoms in molecules allows subdividing molecules into submolecular regions, fragments or single atoms making use of the zero flux surfaces of the electron density gradient vector field $\rho(\boldsymbol{r})$. To evaluate the atomic volumes and charges for the title compound the program TOPXD[25] was used. The atomic volumes V_{tot} are defined by the interatomic boundaries in the crystal. The charge enclosed in V_{tot} is Q_{tot}.

Bader atomic volumes and charges are additive. The sum of atomic volumes in one cell should be equal to the experimental unit cell volume. Similarly the sum of all atomic charges should add up to zero. Summation for trialanine shows that the integration routine has worked properly as the experimental volume V_{exp} = 2362.4 Å^3 and ΣV_{tot} = 2345.9 Å^3 differ by less than 1%, and ΣQ_{tot} differs by only 0.04 e from electroneutrality.

Atomic properties like volume and charge are even better suited to investigate transferability. C_α and C_β atoms could indicate a next-next nearest neighbour influence in this respect. The average of C_α volumes V_{tot} is 7.1(2) Å^3 and that of charges Q_{tot} is 0.15(8) e. Differences in spacial demand between the three C_α-type atoms are smaller than 3%, although a difference in BCP-properties was detected for the C_α–N bonds. For C_β type atoms with average volumes and charges V_{tot} of 9.1(5) Å^3 and Q_{tot} 0.18(6) e the extent of transferability of volumes and charges is even more convincing (see Table 5).

Generally speaking, the atomic volumes and charges depend mainly on the atom and its direct neighbours. One can conclude that for a system like trialanine there is no significant next nearest neighbour's influence except for the partly double bonded peptide atoms. These results encourage a broader use of invarioms, which were recently introduced.[5]

Table 5 Atomic charges (e) and volumes (Å^3) of C_α and C_β atoms with various neighbours. The neighbour type atoms are in parentheses

Atom type	Atom	Q_{tot}	V_{tot}
(N_{amn})–C_α–(C_{pep})	C(2)	0.07	7.34
	C(12)	0.04	7.43
	Average	*0.06*	*7.39*
(N_{pep})–C_α–(C_{pep})	C(8)	0.16	7.05
	C(18)	0.19	6.88
	Average	*0.18*	*6.97*
(N_{pep})–C_α–(C_{carbox})	C(5)	0.17	7.01
	C(15)	0.27	6.77
	Average	*0.22*	*6.89*
C_β–(C_α–NH_3)	C(2A)	0.25	8.93
	C(12A)	0.26	8.40
	Average	*0.26*	*8.67*
C_β–(C_α–N_{pep})	C(5A)	0.09	9.35
	C(15A)	0.16	8.68
	Average	*0.13*	*9.01*
C_β–(C_α–N_{carbox})	C(8A)	0.17	9.66
	C(18A)	0.13	9.58
	Average	*0.20*	*9.62*

Comparison to related studies

The atomic properties derived from trialanine are compared to previous studies of peptides (Table 6). The atoms considered belong to the peptide bond, the carboxylate group and the ammonium group. Within the error limits, charges are mostly the same and volumes are close. For the formally charged carboxylate

Table 6 Averaged atomic charges (e) and volumes (Å^3) of trialanine compared to previous peptides[22]

Atom	V_{tot}[22]	Q_{tot}[22]	V_{tot} Trialanine	Q_{tot} Trialanine
$N_{peptide}$	13(2)	−1.0(2)	13.8(5)	−1.03(3)
$C_{peptide}$	7.0(7)	0.99(9)	6.0(1)	1.1(4)
$O_{peptide}$	20(2)	−0.85(6)	18(1)	−1.13(3)
$O_{carbox,long}$	18(3)	−1.0(2)	16.9(3)	−1.02(4)
$O_{carbox,short}$	16.5(9)	−0.9(2)	20.4(2)	−1.00(4)
C_{carbox}	6.4(6)	1.4(2)	6.1(3)	1.17(5)
$N_{ammonium}$	13(1)	−0.79(9)	15.5(4)	−1.2(1)

and ammonium groups the values of V_{tot} and Q_{tot} deviate more strongly than for the peptide bond. This is due to differences in the hydrogen bonding pattern in the different crystallographic environments that may attenuate the charge located at O_{carbox} and $N_{ammonium}$. These differences influence the corresponding volumes as well. This also holds for the peptide bond, where the effect evoked from hydrogen bonding is about the same size for all of them. As hydrogen atoms are also direct neighbours to oxygen or nitrogen atoms, although not considered covalently bonded, it would be desirable to include a distance dependent influence of hydrogen bonds in invariom modeling.

Hydrogen Bonding

As mentioned above, 12 N–H $\cdots$ O and O–H $\cdots$ O hydrogen bonds (HBs) were found in the asymmetric unit (see Table 2, dashed lines in Fig. 3). For the HB N(11)–H(11C) $\cdots$ O(9B), having the shortest hydrogen–acceptor distance, the influence of this interaction is illustrated qualitatively in the static map shown in Fig. 4. The charge rearrangement in one lone pair lobe of the accepting O(9B) atom is clearly visible.

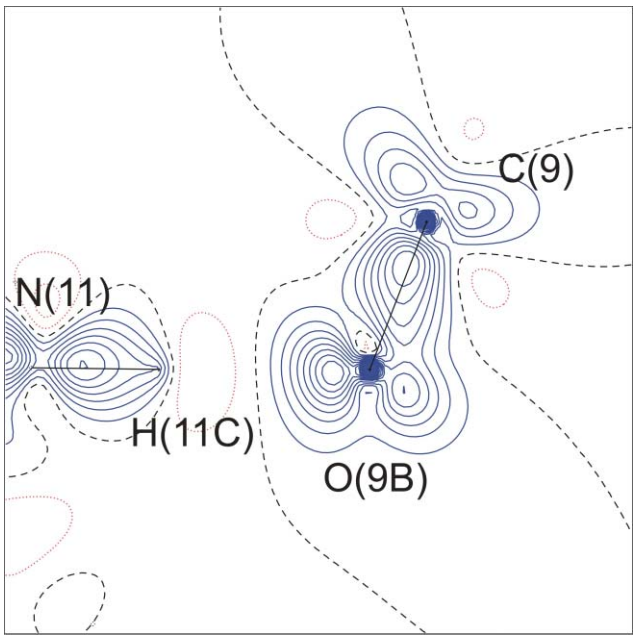

Fig. 4 Static deformation density map in the plane of the strong hydrogen bond N(11)–H(11C) $\cdots$ O(9B), illustrating the charge rearrangement in one of the lone pair lobes of the accepting O(9B) atom, contour intervals 0.1 *e* Å^{-3}.

The influence of hydrogen bonding on the experimental charge density was also studied quantitatively by means of topological properties. Table 2 lists bond critical point properties on the 12 HBs. A relatively low value of the electron density and a positive Laplacian at the BCPs, observed in all cases, are indicative for closed-shell-interactions. Espinosa *et al.*[26] as well as Desiraju and Steiner[27] established an exponential correlation between geometrical and topological parameters. As an example, the experimental hydrogen bond values $\rho(\boldsymbol{r}_{CP})$ and $\nabla^2\rho(\boldsymbol{r}_{CP})$ of trialanine are plotted *versus* the H $\cdots$ A distances in Fig. 5 together with the Espinosa exponential curves. Both the experimental $\rho(\boldsymbol{r})$ and $\nabla^2\rho(\boldsymbol{r})$ values follow rather closely the Espinosa relation. The HB energies E_{HB}, calculated with the relation given by Espinosa *et al.*[28] ($E_{HB} = 25300 \times \exp[-3.6 \times (H \cdots A)]$, kJ mol^{-1}, see last column in Table 2) show that the 12 HBs fall roughly into two groups of six, the stronger ones with $E_{HB} > 40$ kJ mol^{-1} and the weaker ones having $E_{HB} < 30$ kJ mol^{-1}. It is interesting to note that five of the six weaker HBs are involved in establishing the β-sheet type packing of the two independent peptide units (see also Fig. 3) while on the other hand the stronger HBs contribute mainly to the stabilisation of the crystal lattice in other directions.

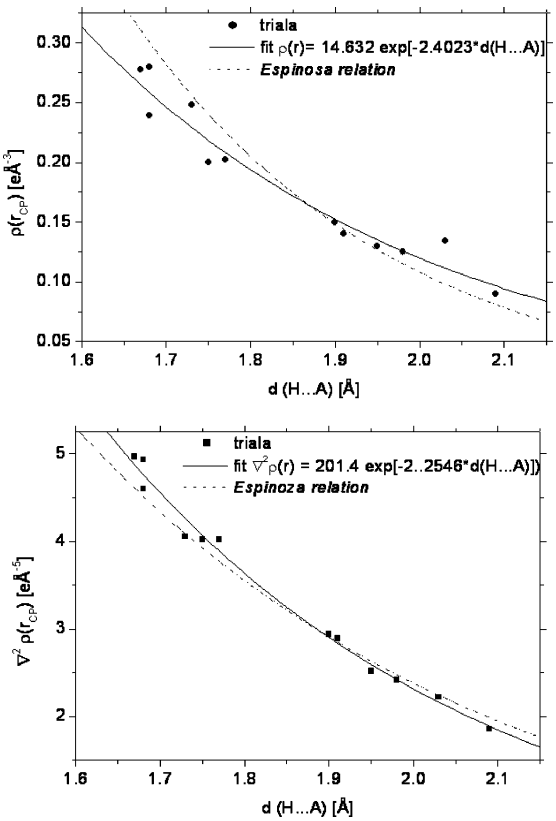

Fig. 5 Hydrogen bond $\rho(\boldsymbol{r}_{CP})$ and $\nabla^2\rho(\boldsymbol{r}_{CP})$ values of trialanine plotted *versus* the d(H $\cdots$ A) distances, fitted according to Espinosa[26] by an exponential curve. The Espinosa relation is also shown for comparison.

Nonbonded valence shell charge concentrations (VSCCs), identified as (3,+3) critical points of $\nabla^2\rho(\boldsymbol{r})$ can be interpreted as the free electron pairs of the valence shell electron pair repulsion (VSEPR) model (orange color in Fig. 3). All theoretically expected VSCCs of the oxygen atoms were determined. The geometric arrangement of the lone pairs is given in Table 7 by the CP–X distance, the angles CP_1–X–CP_2 and X′–X–CP. The CP_1–X–CP_2 angle is generally more than 10° larger than the X′–X–CP angle, which is in accord with the VSEPR model.[29,30] It postulates a higher steric demand for lone-pair electrons than for bonded electron pairs. In the crystalline density the locations of nonbonded VSCCs scatter in a wide range, as expressed by the large variety of CP_1–X–CP_2 (114–157°) and X′–X–CP angles (90–134°). These findings reflect the strong impact of intermolecular influences in the crystalline environment. Similar observations were already made for the VSCCs in our study on six amino acids.[21]

Table 7 Nonbonded valence shell charge concentrations (VSCC). r_{X-CP} denotes the distance of the (3,+3) critical point of $\nabla^2\rho(\boldsymbol{r})$ to the corresponding atom X, X′–X–CP is the angle which is defined by the X′–X and X–CP vectors. CP_1–X–CP_2 is the angle defined by the CP_1–X and X–CP_2 vectors. Units: ρ (e Å^{-3}), $\nabla^2\rho(e$ Å^{-5}), distances (Å) and angles (°)

Atom X	$\rho(\boldsymbol{r})$	$\nabla^2\rho(\boldsymbol{r})$	r_{X-CP}	X′–X–CP	Angle	CP_1–X–CP_2
O(3A)	6.58	−154	0.339	C(3)–O(3A)–CP	110.93	
O(3A)	6.27	−133	0.342	C(3)–O(3A)–CP	108.84	140.12
O(13A)	6.40	−141	0.340	C(13)–O(13)–CP	112.30	
O(13A)	6.23	−125	0.343	C(13)–O(13)–CP	107.99	139.65
O(6A)	6.58	−149	0.339	C(6)–O(6A)–CP	112.66	
O(6A)	6.43	−144	0.340	C(6)–O(6A)–CP	110.92	136.25
O(16A)	6.61	−150	0.338	C(16)–O(16)–CP	116.97	
O(16A)	6.32	−134	0.342	C(16)–O(16)–CP	110.87	132.06
O(9A)	6.21	−125	0.342	C(9)–O(9A)–CP	108.07	
O(9A)	6.35	−133	0.341	C(9)–O(9A)–CP	119.08	132.65
O(9B)	6.62	−157	0.338	C(9)–O(9B)–CP	115.44	
O(9B)	6.31	−138	0.341	C(9)–O(9B)–CP	104.17	140.35
O(19A)	6.37	−133	0.341	C(19)–O(19A)–CP	133.74	
O(19A)	6.40	−148	0.341	C(19)–O(19A)–CP	103.26	113.63
O(19B)	6.42	−142	0.339	C(19)–O(19B)–CP	112.67	
O(19B)	6.44	−145	0.339	C(19)–O(19B)–CP	99.48	147.47
O(21)	5.91	−117	0.346	H(21)–O(21)–CP	89.93	
O(21)	5.89	−117	0.346	H(21)–O(21)–CP	108.60	146.81
O(31)	6.05	−122	0.345	H(31)–O(31)–CP	103.74	
O(31)	6.06	−122	0.345	H(31)–O(31)–CP	90.41	157.46

Conclusion

This study investigates the limits of transferability by experiment. A full topological analysis of the experimental charge density $\rho(\boldsymbol{r})$ of the tripeptide L-alanyl–L-alanyl–L-alanine (trialanine) has been performed and bond topological and integrated atomic properties were determined. For data collection a new setup was used that allows even long lasting area detection experiments at very low temperatures, here 20 K.

Since two conformers are found in the asymmetric unit, the two ammonium groups, two carboxylate groups and four peptide bonds were compared to previous studies on oligopeptides and amino acids. Topological properties of $\rho(\boldsymbol{r})$ and $\nabla^2\rho(\boldsymbol{r})$ were within the error range of these previous studies, so were atomic charges and volumes. A significant detectable influence of next nearest neighbours on the electron density of the C_α and C_β type atoms was not found in the title molecule. The effect remains to be explored for partly double bonded systems. Generally this study shows the validity of the nearest/next-nearest neighbour approximation and supports the use of database approaches for modeling of larger systems or low resolution data. Still multipole refinements on high resolution data sets remain necessary when fine details of hydrogen bonding and crystal field effects are the subject of interest.

Crystal structure data

The tripeptide L-alanyl–L-alanyl-–L-alanine was purchased from Sigma-Aldrich and crystallized from a mixture of dimethylformamide (DMF) and water.

$C_9H_{17}N_3O_4$ x $\frac{1}{2}$ H_2O, Mr = 243.3 g mol^{-1}, monoclinic, a = 18.441(2), b = 5.215(1), c = 24.854(3)Å, β = 98.77(2)°, V = 2362.4(5)Å^3, T = 20 K, space group $C2$ (No. 5), Z = 8, ρ_x = 1.35 g cm^{-3}, μ (Mo Kα) = 1.08 cm^{-1}, $(\sin\theta/\lambda)_{max}$ = 1.15 Å^{-1}, collected/unique reflections 85281/14895, reflections $>4\sigma(F_o)$ 12928, completeness 93.3%, redundancy 5,7, R_{int} = 0.0295, R_1 (spherical) = 0.0289. For further data after multipole refinement, see Table 1.

Acknowledgements

We thank the Deutsche Forschungsgemeinschaft (DFG) for financial support of this work (grant Lu 222/27-1) and the Australian Synchrotron Research Program, which is funded by the Commonealth of Australia under the Major National Research Facilities Program.

References

1 R. F. W. Bader, *Atoms in Molecules*, Clarendon Press, Oxford, 1994.
2 T. Koritsánszky, A. Volkov and P. Coppens, *Acta Crystallogr., Sect. A: Fundam. Crystallogr.*, 2002, **A58**, 464–472.
3 V. Pichon-Pesme, C. Lecomte and H. Lachekar, *J. Phys. Chem. B*, 1995, **99**, 6242–6250.
4 A. Volkov, X. Li, T. Koritsánszky and P. Coppens, *J. Phys. Chem. A*, 2004, **108**, 4283–4300.
5 B. Dittrich, T. Koritsánszky and P. Luger, *Angew. Chem., Int. Ed.*, 2004, **43**, 2718–2721.
6 A. Hempel, N. Camerman and A. Camerman, *Biopolymers*, 1991, **31**(2), 187–192.
7 J. K. Fawcett and N. Camerman, *Acta Crystallogr., Sect. B: Struct. Crystallogr. Cryst. Chem.*, 1975, **31**, 658–665.
8 ORTEP/PLATON:A. L. Spek, *Acta Crystallogr., Sect. A: Fundam. Crystallogr.*, 1990, **46**, A46.
9 M. Messerschmidt, M. Meyer and P. Luger, *J. Appl. Crystallogr.*, 2003, **36**, 1452–1454.
10 *SMART, SAINT, COSMO*: Bruker-AXS Inc., Madison, USA.
11 G. M. Sheldrick, *SHELXS-97, Program for solution of crystal structures*, University of Göttingen, Germany, 1997.
12 N. K. Hansen and P. Coppens, *Acta Crystallogr., Sect. A: Cryst. Phys., Diffr., Theor. Gen. Cryst.*, 1978, **34**, 909–921.
13 T. Koritsánszky, R. P. Mallinson, S. T. Howard, A. Volkov, P. Macchi, Z. Su, C. Gatti, T. Richter, L. J. Farrugia and N. K. Hansen, *XD-A Computer Program for Multipole Refinement and Analysis of Electron Densities from Diffraction Data*, 2003, Manual version 12.
14 M. J. Frisch, G. W. Trucks, H. B. Schlegel, G. E. Scuseria, M. A. Robb, J. R. Cheeseman, V. G. Zakrzewski, J. A. Montgomery, Jr., R. E. Stratmann, J. C. Burant, S. Dapprich, J. M. Millam, A. D. Daniels, K. N. Kudin, M. C. Strain, O. Farkas, J. Tomasi, V. Barone, M. Cossi, R. Cammi, B. Mennucci, C. Pomelli, C. Adamo, S. Clifford, J. Ochterski, G. A. Petersson, P. Y. Ayala, Q. Cui, K. Morokuma, P. Salvador, J. J. Dannenberg, D. K. Malick, A. D. Rabuck, K. Raghavachari, J. B. Foresman, J. Cioslowski, J. V. Ortiz, A. G. Baboul,

B. B. Stefanov, G. Liu, A. Liashenko, P. Piskorz, I. Komaromi, R. Gomperts, R. L. Martin, D. J. Fox, T. Keith, M. A. Al-Laham, C. Y. Peng, A. Nanayakkara, M. Challacombe, P. M. W. Gill, B. G. Johnson, W. Chen, M. W. Wong, J. L. Andres, C. Gonzalez, M. Head-Gordon, E. S. Replogle and J. A. Pople, *GAUSSIAN 98 (Revision A.11)*, Gaussian, Inc., Pittsburgh, PA, 2001.
15 *MORPHY98*: P. L. A. Popelier and R. G. A. Boner, UMIST, Manchester, England, 1998.
16 MOLDEN:G. Schaftenaar and J. H. Noordik, *J. Comput. Aided Mol. Des.*, 2000, **14**, 123–134.
17 *SCHAKAL99*: E. Keller and J. S. Pierrard, Albert-Ludwigs-Universityof Freiburg, Germany, 1999.
18 B. Dittrich, C. B. Hübschle, M. Messerschmidt, R. Kalinowski, D. Girnt and P. Luger, *Acta Crystallogr., Sect. A: Fundam. Crystallogr.*, 2005, **61**, 314–320.
19 D. E. Hibbs, J. Overgaard, S. T. Howard and T. H. Nguyen, *Org. Biomol. Chem.*, 2005, **3**, 441–447.
20 V. Pichon-Pesme, H. Lachekar, M. Souhassou and C. Lecomte, *Acta Crystallogr., Sect. B: Struct. Sci.*, 2000, **56**, 728–737.
21 R. Flaig, T. Koritsánszky, B. Dittrich, A. Wagner and P. Luger, *J. Am. Chem. Soc.*, 2000, **124**, 3407–3417.
22 B. Dittrich, *Herleitung atomarer Eigenschaften von Oligopeptiden aus ihren experimentellen Elektronendichten*, 2002, Ph.D. thesis, Freie Universität Berlin, Berlin.
23 C. Gatti, R. Bianchi, R. Destro and F. Merati, *THEOCHEM*, 1992, **255**, 409–433.
24 B. Dittrich, T. Koritsánszky, M. Grosche, W. Scherer, R. Flaig, A. Wagner, H. G. Krane, H. Kessler, C. Riemer, A. M. M. Scheurs and P. Luger, *Acta Crystallogr., Sect. B: Struct. Sci.*, 2002, **58**, 721–727.
25 TOPXD:A. Volkov, C. Gatti, Y. Abramov and P. Coppens, *Acta Crystallogr., Sect. A: Fundam. Crystallogr.*, 2000, **56**, 252–258.
26 E. Espinosa, M. Souhassou, H. Lachekar and C. Lecomte, *Acta Crystallogr., Sect. B: Struct. Sci.*, 1999, **55**, 563–572.
27 G. Desiraju and T. Steiner, *The Weak Hydrogen Bond*, Oxford University Press, 2001.
28 E. Espinosa, E. Molins and C. Lecomte, *Chem. Phys. Lett.*, 1998, **285**, 170–173.
29 R. J. Gillespie, *Molecular Geometry*, Van Nostrand Reinhold, London, 1972.
30 R. F. W. Bader, R. J. Gillespie and P. J. MacDougall, *J. Am. Chem. Soc.*, 1988, **110**, 7329–7336.